Acta Cryst. (1975). A31, 197

On the Resolution of Slow-Neutron Spectrometers. III. Experimental Test of the Time-of-Flight Diffractometer Resolution-Function Calculations

BY M. POPOVICI AND A.D. STOICA
Institute for Atomic Physics, Bucharest, P.O. Box 35, Romania

AND A. BAJOREK
Joint Institute of Nuclear Research, Dubna, U.S.S.R.

(*Received* 30 *May* 1974; *accepted* 12 *August* 1974)

Experimental determinations of the resolution function of a neutron time-of-flight diffractometer are compared with computations performed within and beyond the normal approximation.

Introduction

For time-of-flight (TOF) neutron diffractometry, the resolution function $R(\mathbf{X})$ defined in the scattering-vector $\mathbf{Q}$ space has been calculated in the preceding paper (Stoica, 1975*b*) which we shall refer to as paper II. The method used there has been described in paper I of this series (Stoica, 1975*a*). This method has two salient features in comparison with the usual technique of computing resolution functions in neutron spectrometry (*e.g.* Cooper & Nathans, 1967, 1968). Firstly, it operates equally well with spatial and angular distributions, so that spatial effects can be accounted for (these effects are lost in the usual technique which operates with angular distributions only). Secondly, it gives a general prescription for calculating the resolution-function moments of any order. The normal approximation is obtained as the simplest approximation involving second-order moments only. By using higher-order moments better approximations can be constructed without difficulty.

In this paper experimental determinations of the TOF diffractometer resolution function are presented and discussed in the context of the mentioned peculiarities of the computation method.

1. The experimental arrangement

The measurements were performed in a TOF diffraction set-up mounted at the pulsed reactor IBR-30 in Dubna on the KDSOG-1 spectrometer. The neutron beam was extracted at an angle of 12° from the surface of a room-temperature water moderator of 30×40 cm area. The sample goniometer was located at a distance $L_1=30$ m from the moderator. The detector of 3 cm diameter was mounted vertically at a distance $L_2=1{\cdot}2$ m from the sample. No Soller collimators were used.

The parameters entering the resolution calculations are the geometry of the experimental arrangement, presented above, and the time dispersion of the thermal neutron pulse as a function of neutron energy. Concerning the latter, there are no explicit theoretical predictions for the intermediate energy range of interest and one has to rely on experimental determinations.

The thermal-neutron pulse is a convolution of the fast-neutron pulse (of dispersion σ_r^2) with the moderator response, so that its dispersion $\langle t^2\rangle$ has the form $\langle t^2\rangle=\sigma_r^2+\sigma_m^2$ where σ_m^2 is the time dispersion of the moderator response function. To determine the energy dependence of σ_m^2 the experimental data of Ishmaev, Sadikov & Chernyshov (1970, 1973) obtained on mockups of the IBR-30 moderators were used. In the search for an empirical interpolation formula for use in the computations, it was found that the available experimental data can be approximated by expressions of the form $\sigma_m=\tau_0[1-\exp(-\lambda/\lambda_0)]$ where λ is the neutron wavelength and τ_0 and λ_0 are adjustable parameters (these expressions have correct asymptotic behaviour: in the limit $\lambda\rightarrow 0$, in the slowing-down transient region, σ_m is proportional to λ, while at large wavelengths, where diffusion becomes the dominant process in the moderator, σ_m approaches a constant value). By fitting the data corresponding to the moderator used in the experiment the values $\tau_0=64$ μsec and $\lambda_0=1{\cdot}6$ Å were obtained. To determine the fast-neutron pulse dispersion the diffraction pattern of a powder Ni sample was measured under nearly focusing conditions (*i.e.* the widths of the Bragg peaks were dominated by the time component of the resolution). By fitting the corrected dispersions (geometry contribution subtracted) of the resolved peaks with the expression $\langle t^2\rangle=\sigma_r^2+\sigma_m^2$ the value $\sigma_r=65$ μsec was obtained (this figure actually includes a contribution due to the jitter of the time-analyser starting pulse with respect to the fast-neutron pulse). More information on the experimental procedure and computation programs may be found in a detailed report (Bajorek, Gheorghiu, Korneev, Kula, Popovici & Stoica, 1974).

2. Computations

The normal approximation

In the normal approximation the actual resolution function is replaced by the three-dimensional Gaussian

$R_G(\mathbf{X})$ having the same covariance matrix:

$$R_G(\mathbf{X}) = R_0 \frac{|\{M_{ij}\}|^{1/2}}{(2\pi)^{3/2}} \exp\left(-\tfrac{1}{2} \sum_{i,j=1}^{3} M_{ij} X_i X_j\right). \quad (1)$$

The explicit expressions for the covariance matrix elements $\langle X_i X_j \rangle$ are given in paper II and can be used as such in computations. The computation program is more flexible, however, if the matrix language is used throughout. The computations reported below were performed with a program based on standard subroutines of matrix multiplication and inversion. The covariance matrix $\mathbf{M}^{-1}$ was computed through the relation $\mathbf{M}^{-1} = \mathbf{T}_2\mathbf{T}_1\mathbf{E}_2\mathbf{T}_1'\mathbf{T}_2'$ where $\mathbf{E}_2$ is the covariance matrix of the original parameters (see paper II) and the matrices $\mathbf{T}_1$ and $\mathbf{T}_2$ are defined by the relations given in Appendices 1 and 2 of paper II. This procedure has the additional advantage of allowing the inclusion at an intermediate stage of the case when Soller collimators and/or neutron guides are used.

Beyond the normal approximation

There are two major reasons for the resolution function to deviate from the Gaussian form in the case under consideration. Firstly, the shape of the thermal neutron pulse is asymmetric. The asymmetry is described quantitatively by the third-order moment $\langle t^3 \rangle$. A non-zero value of $\langle t^3 \rangle$ implies a non-zero third-order moment $\langle X_1^3 \rangle$ of the resolution function. Secondly, the shapes of the moderator, sample and detector are only approximately described by Gaussian distributions of the corresponding coordinates in real space. The actual distributions have flat maxima and this implies a flattening of the resolution-function maximum. The effect is more pronounced in the direction of the X_3 coordinate, because of the considerable vertical extent of the moderator and detector. To account for this effect the fourth-order moments $\langle z_h^4 \rangle$ of the actual distributions should be included in the calculations ($h = 0, 1, 2$ refer to the moderator, sample and detector respectively). These moments will contribute to the fourth moment $\langle X_3^4 \rangle$ only.

The above discussion suggests that the deviations of the resolution function from the Gaussian form could be characterized by two higher-order moments only, $\langle X_1^3 \rangle$ and $\langle X_3^4 \rangle$. Whether this is enough or not will be shown by the experimental results presented in the next section.

The procedure of going to better approximations by considering higher-order moments has been described in paper I for the general case. For the case under consideration it leads to the following result:

$$R(\mathbf{X}) = R_G(\mathbf{X}) \,.\, P(X_1, X_2) \,.\, P_V(X_3) \quad (2)$$

where $R_G(\mathbf{X})$ is the Gaussian approximation (1). The explicit expressions of the polynomials $P(X_1, X_2)$ and $P_V(X_3)$ are obtained by adjusting the coefficients of an expansion in Hermite polynomials. In this way one obtains for $P(X_1, X_2)$ the expression:

$$P(X_1, X_2) = 1 - (\langle X_1^3 \rangle/2) M_{11}(M_{11}X_1 + M_{12}X_2) + (\langle X_1^3 \rangle/6)\,(M_{11}X_1 + M_{12}X_2)^3 \,. \quad (3)$$

By taking into account only the contribution to $\langle X_1^3 \rangle$ due to the asymmetry of the thermal-neutron pulse one has $\langle X_1^3 \rangle = Q_0^3 \langle t^3 \rangle / T_0^3$ (other contributions come from the variation of the incident-neutron spectrum over the resolution range and from the wavelength dependence of the absorption in the detector, but these may be shown to be less important).

The expression of $P_V(X_3)$ is obtained in the form:

$$P_V(X_3) = 1 - (\tfrac{1}{24})\,(3 - M_{33}^2 \langle X_3^4 \rangle)\,(3 - 6M_{33}X_3^2 + M_{33}^2 X_3^4) \quad (4)$$

where $\langle X_3^4 \rangle$ is given by the expression:

$$\langle X_3^4 \rangle = k_{i0}^4 \langle L_1^{-4} \langle z_0^4 \rangle + (L_1^{-1} + L_2^{-1})^4 \langle z_1^4 \rangle + L_2^{-4} \langle z_2^4 \rangle + 6(L_1^{-1} + L_2^{-1})^2 \langle z_1^2 \rangle (L_1^{-2} \langle z_0^2 \rangle + L_2^{-2} \langle z_2^2 \rangle) + 6 L_1^{-2} \langle z_0^2 \rangle L_2^{-2} \langle z_2^2 \rangle] \,.$$

3. Experiment

Method

The method of scanning through $R(\mathbf{X})$ with the aid of Bragg reflexion from perfect single crystals (Dietrich & Als-Nielsen, 1966) has been used in the measurements. The intensity of the neutrons diffracted by a perfect crystal is $I(\mathbf{Q}) \propto R(\mathbf{Q}_0 - \mathbf{Q})$, where $\mathbf{Q}_0 = -2\pi\boldsymbol{\tau}$, $\boldsymbol{\tau}$ being the reciprocal-lattice vector corresponding to the measured Bragg spot. If the angular deviations from the Bragg position in the horizontal (scattering) and vertical planes are denoted by φ and ψ respectively, and the deviation from the mean time-of-flight T_0 by $T - T_0$, then the components of the vector $\mathbf{X} = \mathbf{Q}_0 - \mathbf{Q}$ are: $X_1 = Q_0(T - T_0)/T_0$, $X_2 = Q_0\varphi$ and $X_3 = Q_0\psi$. Therefore, the dependence of the scattered intensity on

Table 1. *Measured and computed data on the covariance matrix* $\{\langle X_i X_j \rangle\}$

Bragg angle −42·5°, perfect Si sample, orders of reflexion 1 to 5.

Q_0 (Å^{-1})	$\langle X_1^2 \rangle$ (Å^{-2})		$\langle X_2^2 \rangle$ (Å^{-2})		$\langle X_1 X_2 \rangle$ (Å^{-2})		$\langle X_3^2 \rangle$ (Å^{-2})		$\lvert\{\langle X_i X_j \rangle\}\rvert^{1/2}$ (Å^{-3})	
	meas.	comp.	meas.	comp.	meas.	comp.	meas.	comp.	meas.	comp.
2·0	9·3E−5	9·3E−5	6·3E−5	6·3E−5	−5·7E−5	−5·2E−5	1·1E−3	1·1E−3	1·7E−6	1·8E−6
8·0	6·6E−3	5·9E−3	1·0E−3	1·0E−3	−6·0E−4	−8·4E−4	1·8E−2	1·8E−2	3·4E−4	3·0E−4
10·0	1·2E−2	1·3E−2	1·6E−3	1·6E−3	−1·0E−3	−1·3E−3	2·7E−2	2·7E−2	7·2E−4	7·1E−4
6·0	2·2E−3	2·2E−3	5·6E−4	5·6E−4	−3·9E−4	−4·7E−4	1·0E−2	1·0E−2	1·1E−4	1·0E−4

$T-T_0$, φ and ψ corresponds to scans through $R(\mathbf{X})$ along three reciprocally perpendicular directions in **Q**-space. The situation is simpler than in conventional diffraction, where the directions corresponding to the θ and φ scans are not perpendicular.

Results

Time-of-flight spectra of neutrons diffracted by the (*nnn*) planes of a perfect Si sample were measured for different deviation angles φ and ψ [the sample was a thin slab of 3·5 cm diameter with (111) planes parallel to the surface, kindly supplied by Dr B. Chalupa]. The two-dimensional arrays of data were analysed to extract corrected sample moments of order up to four. The following data have been compared with calculations: (*a*) the second-order moments $\langle X_i X_j \rangle$; (*b*) the scans along X_1, X_2 and X_3; and (*c*) the contours at 0·5 level of the resolution function in the planes X_1, X_2 and X_1, X_3.

The experimental and computed data on the second-order moments for a Bragg angle of $-42{\cdot}5°$ are given in Table 1. The last two entries in Table 1 are the measured and computed values of the square root of the covariance-matrix determinant, a quantity which is proportional to the resolution volume in **Q** space. It is worth mentioning the fairly good agreement between the measured and computed figures in Table 1 for a resolution volume variation of almost three orders of magnitude. This is essentially due to the proper description of the spatial effects. Note that there were no adjustable parameters in the computation: the geometry of the experiment was known, and the time dispersion of the neutron pulse was determined separately as described in § 1. It is well known that in order to fit to experiment the expressions given by the usual computation technique operating with angular distributions only, one has to introduce 'effective values' of the parameters involved, which often differ considerably from the actual values.

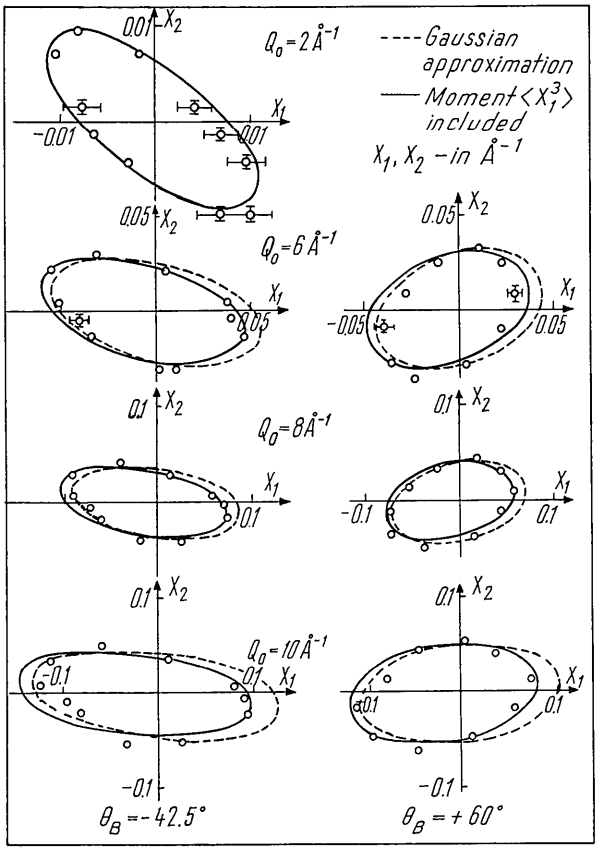

Fig. 2. Experimental and computed contours at 0·5 level of the TOF resolution function in the X_1X_2 plane. Note the different scales for different Q_0 values.

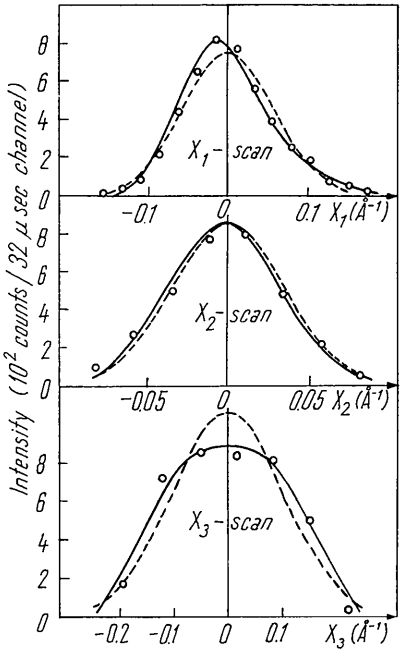

Fig. 1. Scattered neutron intensity corresponding to scans through the resolution function along X_1, X_2 and X_3, for $\theta_B=60°$ and $Q_0=8$ Å^{-1} (reflexion 444 from the perfect Si crystal). Broken lines – Gaussian approximation, full lines – higher-order moments included. Except for normalization to area, calculated curves are not adjusted to the experimental points.

To visualize the actual shape of the resolution function the scans along X_1, X_2 and X_3 are presented in Fig. 1 for one of the measured Bragg spots. The broken curves represent the Gaussian approximation. The full curves were computed according to relation (2) which includes higher-order moments. A constant value of the third-order moment $\langle t^3 \rangle$ was assumed for the sake of simplicity: $\langle t^3 \rangle = \tau_0^3$. The results in Fig. 1 give a positive answer to the question whether the consideration of only two of the higher-order moments suffices for describing the observed deviations from the Gaussian shape.

The half-maximum contours are presented in Figs. 2 and 3. The normal approximation ellipses are shown

by broken lines. The full curves are calculated by including higher-order moments ($\langle X_1^3 \rangle$ alone for Fig. 2 and both $\langle X_1^3 \rangle$ and $\langle X_3^4 \rangle$ for Fig. 3). The improvement of the agreement between experimental and calculated contours when going beyond the normal approximation is particularly impressive for the data referring to the X_1, X_3 plane. The consideration of the fourth-order moment $\langle X_3^4 \rangle$ turns out to be quite important for reproducing the observed contours in this plane. The full curves in Fig. 3 illustrate the situation and give an idea of the potentialities of the computation method.

Conclusions

The experimental check shows that the calculations reported in this series of papers give a fairly adequate description of reality. The major features of the resolution function are reproduced by the normal approximation alone, while details of shape are described by the improved formulae discussed in this paper. Whether these details are relevant or not depends on the physical problem. For instance, the resolution-function dependence on X_3 is not essential, as a rule, in the true diffraction case, but it is important for the quasielastic scattering. For the case of the time-of-flight diffraction on complex structures, such as the substances of interest for biology, the detailed knowledge of the resolution function with respect to all its variables is anticipated to be of particular interest.

We are much indebted to our colleagues Z. Gheorghiu, D. Korneev and R. Kula for experimental assistance.

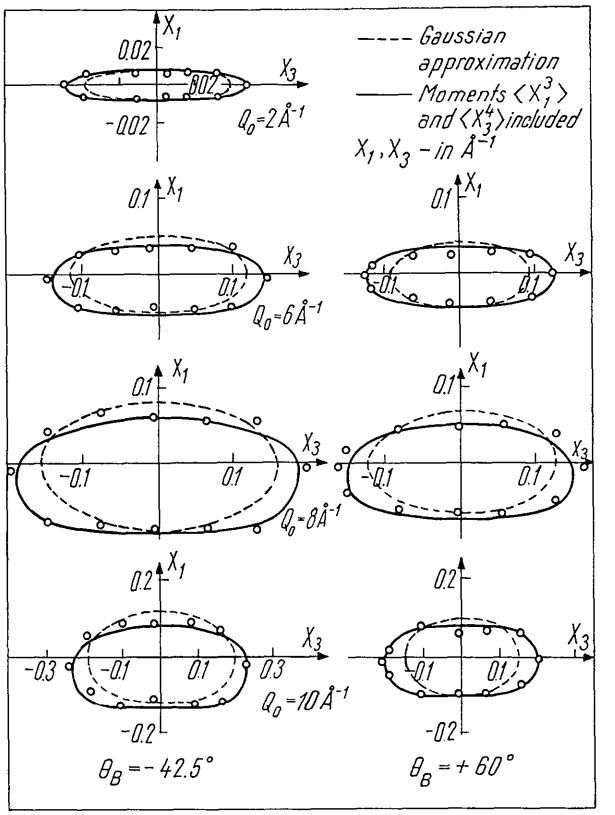

Fig. 3. Experimental and computed data on the contours at 0·5 level of the resolution function in the X_1X_3 plane. Note the different scales for different Q_0 values.

References

BAJOREK, A., GHEORGHIU, Z., KORNEEV, D. A., KULA, R., POPOVICI, M. & STOICA, A. D. (1974). Report JINR (in the press), Joint Institute of Nuclear Research, Dubna.

COOPER, M. J. & NATHANS, R. (1967). *Acta Cryst.* **23**, 357–367.

COOPER, M. J. & NATHANS, R. (1968). *Acta Crvst.* A**24**, 481–484.

DIETRICH, O. W. & ALS-NIELSEN, J. (1966). In *Critical Phenomena*, pp. 144–149. Washington: NBS Miscellaneous Publications 273.

ISHMAEV, S. N., SADIKOV, N. P. & CHERNYSHOV, A. A. (1970). Report IAE-2019, Institute for Atomic Energy, Moscow.

ISHMAEV, S. N., SADIKOV, N. P. & CHERNYSHOV, A. A. (1973). Report IAE-2271, Institute for Atomic Energy, Moscow.

STOICA, A. D. (1975*a*). *Acta Cryst.* A**31**, 189–192.

STOICA, A. D. (1975*b*). *Acta Cryst.* A**31**, 193–196.